# Multiple-Access Bosonic Communications

Brent J. Yen
*Princeton University*
*Department of Electrical Engineering*
*Princeton, New Jersey 08544*

Jeffrey H. Shapiro
*Massachusetts Institute of Technology,*
*Research Laboratory of Electronics*
*Cambridge, Massachusetts 02139*

(Dated: February 1, 2008)

The maximum rates for reliably transmitting classical information over Bosonic multiple-access channels (MACs) are derived when the transmitters are restricted to coherent-state encodings. Inner and outer bounds for the ultimate capacity region of the Bosonic MAC are also presented. It is shown that the sum-rate upper bound is achievable with a coherent-state encoding and that the entire region is asymptotically achievable in the limit of large mean input photon numbers.

PACS numbers: 03.67.Hk, 89.70.+c, 42.79.Sz

## I. INTRODUCTION

The lossy Bosonic channel provides a quantum model for optical communication systems that rely on fiber or free-space propagation. For the pure-loss case, in which the quantum noise accompanying the loss is the minimum permitted by quantum mechanics, the classical information-carrying capacity of this channel has been derived, and shown to be achievable with single-use coherent-state encoding [1]. For the more general thermal-noise channel, in which the environment injects an isotropic Gaussian noise, the Holevo information of single-use coherent-state encoding is a lower bound on the channel capacity that is tight in the limits of low and high noise levels [2, 3]. Moreover, if a recent conjecture concerning the thermal-noise channel's minimum output entropy is correct, then single-use coherent-state encoding is capacity achieving [4].

To date there has been almost nothing reported about the classical information-carrying capacity region of multiple-access Bosonic channels, i.e., Bosonic channels in which two or more senders communicate to a common receiver over a shared propagation medium. In this paper we derive single-mode and wideband capacity results for such channels [5]. First, we show that single-use coherent-state encoding with joint measurements over entire codewords achieves the sum capacity and provides lower bounds on the individual-user capacities. Then we quantify the capacity region that is lost when heterodyne or homodyne detection is employed—in lieu of the optimum joint measurement—with single-use coherent-state encoding. Finally, we derive upper bounds on the individual-user capacities, and show that they can be achieved—in the limit of high input photon numbers—by means of squeezed-state encoding and homodyne detection.

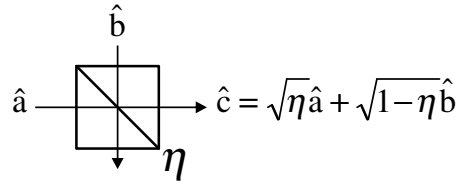


FIG. 1: Two-user, single-mode, optical multiple-access channel. Transmitters Alice and Bob have access to input modes $\hat{a}$ and $\hat{b}$, respectively. Charlie receives the output mode $\hat{c} = \sqrt{\eta}\,\hat{a} + \sqrt{1-\eta}\,\hat{b}$.

## II. COHERENT-STATE MAC

We will begin with the single-mode optical MAC, shown in Fig. 1, in which two senders, Alice and Bob, transmit classical information to a common receiver, Charlie, by accessing different input ports of a lossless beam splitter with transmissivity $\eta$, where $0 \leq \eta \leq 1$. The input-output relation for the electromagnetic modes associated with this channel is $\hat{c} = \sqrt{\eta}\,\hat{a} + \sqrt{1-\eta}\,\hat{b}$, where $\hat{a}$ and $\hat{b}$ are the annihilation operators of Alice's and Bob's input modes, and $\hat{c}$ is the annihilation operator of the mode that Charlie measures. In this section, we derive the capacity of the optical MAC when Alice and Bob encode complex-valued input messages $\alpha$ and $\beta$ as coherent states $|\alpha\rangle_A \otimes |\beta\rangle_B$ with independent probability densities $p_A(\alpha)$ and $p_B(\beta)$. This encoding puts the $\hat{c}$ mode in the coherent state $|\sqrt{\eta}\,\alpha + \sqrt{1-\eta}\,\beta\rangle_C$, so we will refer to this system as the two-user, single-mode, coherent-state MAC.

### A. Quantum MAC Capacity Theorem

The capacity region of a two-user multiple-access channel is defined to be the closure of all rate pairs $(R_1, R_2)$ for which arbitrarily small error probabilities are achievable in the limit of long codewords [6]. Winter's quantum MAC capacity theorem [7] gives the capacity region of a quantum MAC optimized over arbitrary receiver measurements, and over codewords that are not entangled over multiple channel uses. Winter's result presumes a finite-dimensional state space, whereas the Bosonic MAC has an infinite-dimensional state space. Nevertheless, we shall rely on his result, which can be extended to Bosonic channels by means of a limiting argument, see Appendix. Thus, the capacity region of the two-user, single-mode, optical MAC from Fig. 1 will be taken to be the convex closure of all rate pairs $(R_1, R_2)$ that satisfy the following inequalities:

$$R_1 \leq \int p_B(\beta) S(\hat{\rho}_\beta^B)\, \mathrm{d}\beta - \iint p_A(\alpha) p_B(\beta) S(\hat{\rho}(\alpha,\beta))\, \mathrm{d}\alpha\, \mathrm{d}\beta, \tag{1a}$$

$$R_2 \leq \int p_A(\alpha) S(\hat{\rho}_\alpha^A)\, \mathrm{d}\alpha - \iint p_A(\alpha) p_B(\beta) S(\hat{\rho}(\alpha,\beta))\, \mathrm{d}\alpha\, \mathrm{d}\beta, \tag{1b}$$

$$R_1 + R_2 \leq S(\bar{\rho}) - \iint p_A(\alpha) p_B(\beta) S(\hat{\rho}(\alpha,\beta))\, \mathrm{d}\alpha\, \mathrm{d}\beta, \tag{1c}$$

for some product distribution, $p_A(\alpha)p_B(\beta)$, on Alice's and Bob's complex-valued inputs. In these expressions, $S(\cdot)$ is the von Neumann entropy, and the average density operators are

$$\hat{\rho}_\beta^B = \int p_A(\alpha) \hat{\rho}(\alpha,\beta)\, \mathrm{d}\alpha, \tag{2}$$

$$\hat{\rho}_\alpha^A = \int p_B(\beta) \hat{\rho}(\alpha,\beta)\, \mathrm{d}\beta, \tag{3}$$

$$\bar{\rho} = \iint p_A(\alpha) p_B(\beta) \hat{\rho}(\alpha,\beta)\, \mathrm{d}\alpha\, \mathrm{d}\beta, \tag{4}$$

where $\hat{\rho}(\alpha,\beta)$ is the received state given that messages $\alpha$ and $\beta$ have been transmitted. The capacity region will diverge unless the inputs are constrained, so here we assume that Alice and Bob are subject to the average photon-number constraints $\langle \hat{a}^\dagger \hat{a} \rangle \leq \bar{n}_A$ and $\langle \hat{b}^\dagger \hat{b} \rangle \leq \bar{n}_B$, respectively.

Equations (1) constitute the multiple-access version of the Holevo-Schumacher-Westmoreland theorem, which gives the classical capacity of a single-user quantum channel [8, 9, 10]. For the coherent-state MAC, $\hat{\rho}(\alpha,\beta) = |\sqrt{\eta}\,\alpha + \sqrt{1-\eta}\,\beta\rangle\langle\sqrt{\eta}\,\alpha + \sqrt{1-\eta}\,\beta|$ is a pure state, so that the second terms on the right-hand sides of these equations vanish, and the average density operators in the first terms are found by performing the indicated integrations in Eqs. (2)–(4).

### B. Coherent-State MAC Capacity

Suppose that Charlie uses homodyne or heterodyne detection. These are single-use measurements that may not achieve the capacity region of the coherent-state MAC, but they are easily realized with existing technology and their capacity regions are simple to derive. In particular, coherent-state MACs that use homodyne or heterodyne detection reduce to classical additive Gaussian noise MACs: a scalar Gaussian MAC, with noise variance 1/4, for homodyne detection, and a 2D white-Gaussian noise MAC, with noise variance 1/2 per dimension, for heterodyne detection. It follows that the capacity region for the coherent-state MAC with homodyne detection is the set of rate pairs $(R_1, R_2)$ that satisfy [6]

$$R_1 \leq \frac{1}{2}\log(1 + 4\eta\bar{n}_A) \tag{5a}$$

$$R_2 \leq \frac{1}{2}\log(1 + 4(1-\eta)\bar{n}_B) \tag{5b}$$

$$R_1 + R_2 \leq \frac{1}{2}\log(1 + 4\eta\bar{n}_A + 4(1-\eta)\bar{n}_B), \tag{5c}$$

and the capacity region for the coherent-state MAC with heterodyne detection is

$$R_1 \leq \log(1 + \eta\bar{n}_A) \tag{6a}$$

$$R_2 \leq \log(1 + (1-\eta)\bar{n}_B) \tag{6b}$$

$$R_1 + R_2 \leq \log(1 + \eta\bar{n}_A + (1-\eta)\bar{n}_B), \tag{6c}$$

when Alice and Bob are subject to the average photon-number constraints $\bar{n}_A$ and $\bar{n}_B$, respectively.

The preceding two-user results extend easily to the $m$-user coherent-state MAC that employs homodyne or heterodyne detection. Here, the $i$th transmitter sends coherent state $|\alpha_i\rangle$, for $1 \leq i \leq m$, resulting in the channel's output mode being in the coherent state $|\sum_{i=1}^m \sqrt{\eta_i}\,\alpha_i\rangle$, where the transmissivities $\{\eta_i\}$ sum to one. The $m$-user capacity region with homodyne detection is then the set of rates $(R_1, \ldots, R_m)$ that satisfy the inequalities

$$\sum_{i\in S} R_i \leq \frac{1}{2}\log\left(1 + 4\sum_{i\in S}\eta_i\bar{n}_i\right), \tag{7}$$

for all subsets $S \subseteq \{1, \ldots, m\}$, where $\langle \hat{a}_i^\dagger \hat{a}_i \rangle \leq \bar{n}_i$ is the average photon-number constraint on the $i$th user. Similarly, the capacity region with heterodyne detection is given by the inequalities

$$\sum_{i\in S} R_i \leq \log\left(1 + \sum_{i\in S}\eta_i\bar{n}_i\right), \tag{8}$$

for all subsets $S \subseteq \{1, \ldots, m\}$.

The homodyne and heterodyne detection capacity regions for the coherent-state MAC provide inner bounds on that channel's capacity region if no constraints are placed on the receiver measurements. We will now

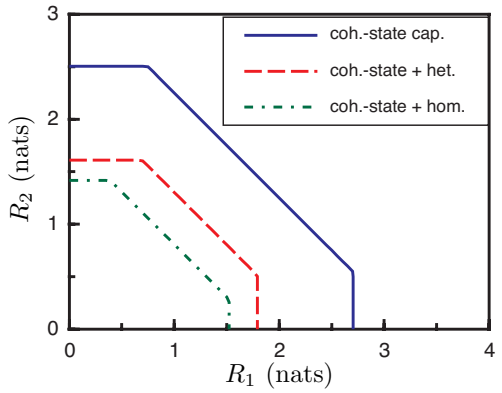


FIG. 2: (Color online) Coherent-state capacity region for the optical MAC. The capacity region with optimum reception (solid line) is given by inequalities (11). The capacity regions with homodyne detection and heterodyne detection are also shown. This figure assumes $\eta = 1/2$, $\bar{n}_A = 10$, and $\bar{n}_B = 8$. Rates are measured in nats, i.e., logarithms are taken base $e$.

find the capacity region for the coherent-state MAC—without restricting the choice of receiver structure—from the previously stated capacity theorem. The channel outputs of the coherent-state MAC are the pure states $\hat{\rho}(\alpha,\beta) = |\sqrt{\eta}\,\alpha + \sqrt{1-\eta}\,\beta\rangle\langle\sqrt{\eta}\,\alpha + \sqrt{1-\eta}\,\beta|$. It is then easy to show that the circularly-symmetric Gaussian distributions

$$p_A(\alpha) = \frac{1}{\pi\bar{n}_A}\exp\left(-\frac{|\alpha|^2}{\bar{n}_A}\right), \tag{9}$$

$$p_B(\beta) = \frac{1}{\pi\bar{n}_B}\exp\left(-\frac{|\beta|^2}{\bar{n}_B}\right), \tag{10}$$

are the optimal input distributions, i.e., they maximize the right–hand sides of (1) for the coherent-state MAC. Using these input distributions we find that the capacity region of the coherent-state MAC, with optimal (joint measurements over entire codewords) reception is the set of all rate pairs satisfying

$$R_1 \le g(\eta\bar{n}_A) \tag{11a}$$

$$R_2 \le g((1-\eta)\bar{n}_B) \tag{11b}$$

$$R_1 + R_2 \le g(\eta\bar{n}_A + (1-\eta)\bar{n}_B), \tag{11c}$$

where $g(x) \equiv (x+1)\log(x+1) - x\log(x)$ is the Shannon entropy of the Bose-Einstein probability distribution. Figure 2 compares the capacity regions for the coherent-state MAC when homodyne detection, heterodyne detection, and optimal reception are used.

Users transmitting information over the optical MAC must each contend with interference created by the other users who are attempting to access the channel. This type of noise, called multiple-access interference, is responsible for the pentagonal shape of the capacity region seen in Fig. 2. In general, users communicating over a multiple-access channel will encounter channel noise in addition to multiple-access interference. A two-user, single-mode, optical MAC that introduces additional white-Gaussian noise can be modeled by the evolution equation $\hat{c} = \sqrt{\eta}\ \hat{a} + \sqrt{1-\eta}\ \hat{b} + \xi$, where $\xi$ is additive classical zero-mean, complex-valued, white-Gaussian noise with variance $\langle|\xi|^2\rangle = N$. Our derivation of the two-user capacity region for the coherent-state MAC generalizes to include the presence of additive white-Gaussian noise, with the following result for the capacity region:

$$R_1 \le g(\eta\bar{n}_A + N) - g(N) \tag{12a}$$

$$R_2 \le g((1-\eta)\bar{n}_B + N) - g(N) \tag{12b}$$

$$R_1 + R_2 \le g(\eta\bar{n}_N + (1-\eta)\bar{n}_B + N) - g(N). \tag{12c}$$

### C. Wideband Capacity

Now let us turn our attention to the wideband coherent-state MAC, in which Alice and Bob may employ photons of any frequency, subject to constraints, $P_A$ and $P_B$, on their average transmitted powers. For a frequency-multiplexed scheme, in which the radian-frequency domain is divided into bins of width $\Delta = 2\pi/T$, the channel output for the $i$th mode is

$$\hat{c}_i = \sqrt{\eta}\,\hat{a}_i + \sqrt{1-\eta}\,\hat{b}_i, \tag{13}$$

where $\hat{a}_i$ and $\hat{b}_i$ are the input modes at frequency $\omega_i = i2\pi/T$, for $i = 1, 2, 3, \ldots$, and the transmissivity $\eta$ is frequency independent. The average power constraints on Alice and Bob are given by

$$\sum_i \hbar\omega_i\langle|\alpha_i|^2\rangle\Delta/2\pi \le P_A \tag{14}$$

$$\sum_i \hbar\omega_i\langle|\beta_i|^2\rangle\Delta/2\pi \le P_B, \tag{15}$$

where Alice and Bob allocate average photon numbers $\bar{n}_A(\omega_i) = \langle|\alpha_i|^2\rangle$ and $\bar{n}_B(\omega_i) = \langle|\beta_i|^2\rangle$, respectively, to frequency-bin $\omega_i$.

We first derive the capacity region of the wideband coherent-state MAC with homodyne detection. When homodyne detection is employed, the wideband coherent-state MAC is equivalent to a set of parallel classical MACs with independent zero-mean Gaussian noise, for which we have derived upper bounds on the individual rates, $R_1$ and $R_2$, and on the sum rate, $R_1 + R_2$, from separate Lagrange multiplier calculations. In the limit $\Delta \to 0$, these upper bounds become

$$R_1 \le \sqrt{\frac{\eta P_A}{\pi\hbar}} \tag{16a}$$

$$R_2 \le \sqrt{\frac{(1-\eta)P_B}{\pi\hbar}} \tag{16b}$$

$$R_1 + R_2 \le \sqrt{\frac{\eta P_A + (1-\eta)P_B}{\pi\hbar}}, \tag{16c}$$

with

$$\eta\bar{n}_A(\omega) = \frac{1}{\omega}\sqrt{\frac{\pi\eta P_A}{\hbar}} - \frac{1}{4}, \tag{17}$$

for $\omega \leq 4\sqrt{\pi\eta P_A/\hbar}$,

$$(1-\eta)\bar{n}_B(\omega) = \frac{1}{\omega}\sqrt{\frac{\pi(1-\eta)P_B}{\hbar}} - \frac{1}{4}, \tag{18}$$

for $\omega \leq 4\sqrt{\pi(1-\eta)P_B/\hbar}$, and

$$\bar{n}'_{AB}(\omega) = \frac{1}{\omega}\sqrt{\frac{\pi[\eta P_A + (1-\eta)P_B]}{\hbar}} - \frac{1}{4}, \tag{19}$$

for $\omega \leq 4\sqrt{\pi[\eta P_A + (1-\eta)P_B]/\hbar}$, where $\bar{n}'_{AB}(\omega) \equiv \eta\bar{n}_A(\omega) + (1-\eta)\bar{n}_B(\omega)$.

We see that the optimal mean photon number allocations, $\bar{n}_A(\omega)$ and $\bar{n}_B(\omega)$, are given by water-filling formulas, as is found in classical information theory. The rates (16) define a pentagonal region which serves as an outer bound for the capacity of the wideband coherent-state MAC with homodyne detection. To prove that this outer bound is, in fact, the capacity region, we must show that Eqs. (17)–(19) can be satisfied simultaneously. The average photon number allocations $(\bar{n}_A(\omega), (\bar{n}'_{AB}(\omega) - \eta\bar{n}_A(\omega))/(1-\eta))$ for Alice and Bob, achieve the lower-right corner point

$$\left(\sqrt{\frac{\eta P_A}{\pi\hbar}},\ \sqrt{\frac{\eta P_A + (1-\eta)P_B}{\pi\hbar}} - \sqrt{\frac{(1-\eta)P_B}{\pi\hbar}}\right) \tag{20}$$

of the outer bound. Similarly, $((\bar{n}'_{AB}(\omega) - (1-\eta)\bar{n}_B(\omega))/\eta, \bar{n}_B(\omega))$ achieves the upper-left corner. Thus, the entire region is achievable and hence is equal to the capacity region. A similar derivation shows that the wideband coherent-state MAC with heterodyne detection has a capacity region that is identical to that of homodyne detection.

The preceding two-user wideband results readily extend to the $m$-user wideband coherent-state MAC. Suppose that the $k$th user sends coherent states $\{|\alpha_{k,i}\rangle\}$ across the frequency bins $\{\omega_i\}$. The channel output for the $i$th-frequency mode will then be the coherent state $|\sum_{k=1}^{m}\sqrt{\eta_k}\alpha_{k,i}\rangle$, where the frequency-independent transmissivities $\eta_k$ sum to one. The input power constraint on the $k$th user is

$$\sum_i \hbar\omega_i\langle|\alpha_{k,i}|^2\rangle\Delta/2\pi \leq P_k, \tag{21}$$

for $1 \leq k \leq m$. If the receiver uses homodyne or heterodyne detection, then the wideband capacity region is defined by the inequalities

$$\sum_{k\in S} R_k \leq \sqrt{\sum_{k\in S}\frac{\eta_k P_k}{\pi\hbar}}, \tag{22}$$

for all $S \subseteq \{1,\ldots,m\}$.

In deriving the wideband capacity region for the two-user, coherent-state MAC with homodyne or heterodyne detection, we first obtained upper bounds on the individual rates $R_1$, $R_2$, and the sum rate $R_1 + R_2$, and then showed that these bounds could be achieved simultaneously. Applying this same procedure to the two-user, coherent-state MAC without constraining its receiver structure, we have obtained the following capacity region,

$$R_1 \leq \sqrt{\frac{\pi\eta P_A}{3\hbar}} \tag{23a}$$

$$R_2 \leq \sqrt{\frac{\pi(1-\eta)P_B}{3\hbar}} \tag{23b}$$

$$R_1 + R_2 \leq \sqrt{\frac{\pi[\eta P_A + (1-\eta)P_B]}{3\hbar}}, \tag{23c}$$

and optimal average photon number allocations,

$$\eta\bar{n}_A(\omega) = \frac{1}{\exp\left(\sqrt{\pi\hbar\omega^2/12\eta P_A}\right) - 1}, \tag{24}$$

$$(1-\eta)\bar{n}_B(\omega) = \frac{1}{\exp\left(\sqrt{\pi\hbar\omega^2/12(1-\eta)P_B}\right) - 1}, \tag{25}$$

$$\bar{n}'_{AB}(\omega) = \frac{1}{\exp\left(\sqrt{\pi\hbar\omega^2/12[\eta P_A + (1-\eta)P_B]}\right) - 1}. \tag{26}$$

Equations (16) and (23) show that optimal reception increases both the individual rates and the sum rate by a factor of $\pi/\sqrt{3}$ as compared to what is achievable with homodyne or heterodyne detection. The $m$-user capacity region for the coherent-state MAC is specified by the inequalities

$$\sum_{k\in S} R_k \leq \sqrt{\sum_{k\in S}\frac{\pi\eta_k P_k}{3\hbar}}, \tag{27}$$

for all $S \subseteq \{1,\ldots,m\}$; once again there is an improvement factor of $\pi/\sqrt{3}$ as compared to homodyne or heterodyne detection.

## III. GAUSSIAN MAC

Now let us return to the single-mode case and relax our assumption that the transmitters use coherent-state encodings, i.e., we will allow them to use non-classical states in their quest for the largest possible capacity region. As a step toward finding the ultimate capacity region of the optical MAC, let us allow Alice and Bob to employ arbitrary Gaussian states, instead of just coherent states.

### A. Holevo-Sohma-Hirota MAC

It is useful to begin by deriving the capacity region for the two-user version of the Holevo-Sohma-Hirota [11]

(HSH) channel model. Consider a mode with annihilation operator $\hat{a} = \hat{a}_1 + i\hat{a}_2$ that is in a zero-mean, Gaussian state, $\hat{\rho}(0)$, with quadrature-component covariance matrix

$$V = \begin{pmatrix} V_1 & V_{12} \\ V_{12} & V_2 \end{pmatrix} \equiv \begin{pmatrix} \langle \hat{a}_1^2 \rangle & \langle \hat{a}_1\hat{a}_2 + \hat{a}_2\hat{a}_1 \rangle/2 \\ \langle \hat{a}_1\hat{a}_2 + \hat{a}_2\hat{a}_1 \rangle/2 & \langle \hat{a}_2^2 \rangle \end{pmatrix}. \tag{28}$$

We define a multiple access channel model in which Alice and Bob send classical messages $\alpha$ and $\beta$, subject to input constraints

$$\langle |\alpha|^2 \rangle \equiv \int |\alpha|^2 p_A(\alpha)\, \mathrm{d}\alpha = N_A, \tag{29}$$

$$\langle |\beta|^2 \rangle \equiv \int |\beta|^2 p_B(\beta)\, \mathrm{d}\beta = N_B, \tag{30}$$

and Charlie receives the shifted version of the initial state, viz., $\hat{\rho}(\alpha, \beta) = \hat{D}(\alpha + \beta)\hat{\rho}(0)\hat{D}^\dagger(\alpha + \beta)$, where $\hat{D}(\gamma) \equiv \exp(\gamma\hat{a}^\dagger - \gamma^*\hat{a})$ is the displacement operator. From the quantum MAC capacity theorem [7], the capacity region of the two-user HSH MAC is given by the convex hull of all rate pairs $(R_1, R_2)$ satisfying

$$R_1 \leq S(\bar{\rho}_A) - S(\hat{\rho}(0)) \tag{31a}$$

$$R_2 \leq S(\bar{\rho}_B) - S(\hat{\rho}(0)) \tag{31b}$$

$$R_1 + R_2 \leq S(\bar{\rho}_{AB}) - S(\hat{\rho}(0)), \tag{31c}$$

for some product distribution $p_A(\alpha)p_B(\beta)$, where the average density operators are

$$\bar{\rho}_A = \int p_A(\alpha)\hat{D}(\alpha)\hat{\rho}(0)\hat{D}^\dagger(\alpha)\, \mathrm{d}\alpha, \tag{32}$$

$$\bar{\rho}_B = \int p_B(\beta)\hat{D}(\beta)\hat{\rho}(0)\hat{D}^\dagger(\beta)\, \mathrm{d}\beta, \tag{33}$$

$$\bar{\rho}_{AB} = \iint p_A(\alpha)p_B(\beta)\hat{\rho}(\alpha, \beta)\, \mathrm{d}\alpha\, \mathrm{d}\beta. \tag{34}$$

To evaluate this capacity region, we will first maximize the rate upper bounds for $R_1$, $R_2$, and $R_1+R_2$ separately. Then we will then show that the region described by these maximum rates is achievable.

To maximize the $R_1$ upper bound in (31a), we follow the proof of the HSH capacity theorem [11]; the same derivation will also apply to the $R_2$ upper bound. For any input distribution $p_A(\alpha)$ that satisfies constraint (29), let $\tilde{p}_A(\alpha)$ be the zero-mean Gaussian distribution with the same second moments as $p_A(\alpha)$. Then, $\tilde{p}_A(\alpha)$ satisfies constraint (29) and

$$\tilde{\rho}_A = \int \tilde{p}_A(\alpha)\hat{D}(\alpha)\hat{\rho}(0)\hat{D}^\dagger(\alpha)\, \mathrm{d}\alpha \tag{35}$$

is a Gaussian state. If $F(\hat{a}, \hat{a}^\dagger)$ is any second-order polynomial in $(\hat{a}, \hat{a}^\dagger)$, then

$$\mathrm{tr}[\bar{\rho}_A F(\hat{a}, \hat{a}^\dagger)] = \int p_A(\alpha)\, \mathrm{tr}[\hat{D}(\alpha)\hat{\rho}(0)\hat{D}^\dagger(\alpha)F(\hat{a}, \hat{a}^\dagger)]\, \mathrm{d}\alpha \tag{36}$$

$$= \int p_A(\alpha)\, \mathrm{tr}[\hat{\rho}(0)F(\hat{a} + \alpha, \hat{a}^\dagger + \alpha^*)]\, \mathrm{d}\alpha \tag{37}$$

$$= \int \tilde{p}_A(\alpha)\, \mathrm{tr}[\hat{\rho}(0)F(\hat{a} + \alpha, \hat{a}^\dagger + \alpha^*)]\, \mathrm{d}\alpha \tag{38}$$

$$= \mathrm{tr}[\tilde{\rho}_A F(\hat{a}, \hat{a}^\dagger)]. \tag{39}$$

Thus, $\bar{\rho}_A$ and $\tilde{\rho}_A$ have the same second moments, and it follows that $S(\tilde{\rho}_A) \geq S(\bar{\rho}_A)$, i.e., we can restrict our attention to Gaussian input distributions in trying to maximize the $R_1$ upper bound.

When the input distribution $p_A(\alpha)$ is Gaussian, the rate upper bound for $R_1$ can be expressed as

$$S(\bar{\rho}_A) - S(\hat{\rho}(0)) = g(2|V + V_\alpha|^{1/2} - 1/2) - g(2|V|^{1/2} - 1/2), \tag{40}$$

where the quadrature-component covariance matrix of $p_A(\alpha)$ is

$$V_\alpha = \begin{pmatrix} V_1^\alpha & V_{12}^\alpha \\ V_{12}^\alpha & V_2^\alpha \end{pmatrix}. \tag{41}$$

Thus, the optimization problem we need to solve is $\max_{V_\alpha} |V + V_\alpha|$, subject to the positive semidefinite and input power constraints

$$V_\alpha \geq 0, \tag{42}$$

$$\mathrm{tr}(V_\alpha) = V_1^\alpha + V_2^\alpha = N_A. \tag{43}$$

This constraint region is the interior of a circle in the $V_1^\alpha - V_{12}^\alpha$ plane, which has the following polar-coordinate parameterization,

$$V_1^\alpha = r\cos\theta + \frac{N_A}{2}, \quad V_{12}^\alpha = r\sin\theta, \quad V_2^\alpha = -r\cos\theta + \frac{N_A}{2}, \tag{44}$$

where $0 \leq r \leq N_A/2$ and $0 \leq \theta < 2\pi$. Now, write

$$|V + V_\alpha| = (V_1 + V_1^\alpha)(V_2 + V_2^\alpha) - (V_{12} + V_{12}^\alpha)^2 \tag{45}$$

$$= \left(\frac{V_1 + V_2 + N_A}{2}\right)^2 - \left(\frac{V_1 - V_2}{2} + r\cos\theta\right)^2 - (V_{12} + r\sin\theta)^2. \tag{46}$$

In terms of $r$ and $\theta$, our maximization problem then becomes

$$\max_{V_\alpha} |V + V_\alpha| = \left(\frac{V_1 + V_2 + N_A}{2}\right)^2 - \min_{r,\theta} \left[\left(\frac{V_2 - V_1}{2} - r\cos\theta\right)^2 + (-V_{12} - r\sin\theta)^2\right]. \tag{47}$$

This maximization has two different solutions, depending on whether or not the point $((V_2 - V_1)/2, -V_{12})$ lies in the radius-$N_A/2$ circle whose center is at the origin. If $((V_2 - V_1)/2, -V_{12})$ lies in this circle, then the minimum on the right-hand side of (47) is zero. If $((V_2 - V_1)/2, -V_{12})$ lies outside this circle, then a simple geometric calculation gives the minimum on the right-hand side of (47). We thus obtain the maximum individual rates

$$R_{\max 1} = \max_{V_\alpha} S(\bar{\rho}_A) - S(\hat{\rho}(0)) \tag{48}$$

$$= \begin{cases} g\big(V_1 + V_2 + N_A - \frac{1}{2}\big) - g\left(2|V|^{1/2} - \frac{1}{2}\right), \\ \qquad \text{for } N_A \geq ((V_1 - V_2)^2 + 4V_{12}^2)^{1/2}, \\ g\left(2\left[[(V_1 + V_2 + N_A)/2]^2 - \left(\sqrt{[(V_1 - V_2)/2]^2 + V_{12}^2} - N_A/2\right)^2\right]^{1/2} - \frac{1}{2}\right) - g\left(2|V|^{1/2} - \frac{1}{2}\right), \\ \qquad \text{for } N_A < ((V_1 - V_2)^2 + 4V_{12}^2)^{1/2} \end{cases} \tag{49}$$

A similar expression holds for the maximum rate $R_{\max 2}$. The fact that capacity is given by two different expressions depending on whether input constraints satisfy a certain inequality is referred to as a noncommutative generalization of waterfilling in [11].

To maximize the sum-rate upper bound, we follow the same approach. It is again sufficient to consider Gaussian input distributions $p_A(\alpha)$ and $p_B(\beta)$, so our maximization problem is $\max_{V_\alpha, V_\beta} |V + V_\alpha + V_\beta|$, subject to the positive semidefinite and input power constraints

$$V_\alpha \geq 0, \quad V_\beta \geq 0, \tag{50}$$

$$\mathrm{tr}(V_\alpha) = V_1^\alpha + V_2^\alpha = N_A, \quad \mathrm{tr}(V_\beta) = V_1^\beta + V_2^\beta = N_B. \tag{51}$$

This constraint region is the interior of two circles whose polar-coordinate parameterizations are

$$V_\alpha = \begin{pmatrix} r_A \cos\theta_A & r_A \sin\theta_A \\ r_A \sin\theta_A & -r_A \cos\theta_A \end{pmatrix} + \frac{N_A}{2} I, \tag{52}$$

$$V_\beta = \begin{pmatrix} r_B \cos\theta_B & r_B \sin\theta_B \\ r_B \sin\theta_B & -r_B \cos\theta_B \end{pmatrix} + \frac{N_B}{2} I, \tag{53}$$

for $0 \leq r_A \leq N_A/2$, $0 \leq r_B \leq N_B/2$, $0 \leq \theta_A < 2\pi$, and $0 \leq \theta_B < 2\pi$, with $I$ being the $2 \times 2$ identity matrix. This parameterization allows us to write

$$\begin{aligned} |V + V_\alpha + V_\beta| &= (V_1 + V_1^\alpha + V_1^\beta)(V_2 + V_2^\alpha + V_2^\beta) \\ &\quad -(V_{12} + V_{12}^\alpha + V_{12}^\beta)^2 \qquad (54) \\ &= \left(\frac{V_1 + V_2 + N_A + N_B}{2}\right)^2 \\ &\quad - \left(\frac{V_1 - V_2}{2} + r_A \cos\theta_A + r_B \cos\theta_B\right)^2 \\ &\quad -(V_{12} + r_A \sin\theta_A + r_B \sin\theta_B)^2. \qquad (55) \end{aligned}$$

Thus, we have

$$\begin{aligned} &\max_{V_\alpha, V_\beta} |V + V_\alpha + V_\beta| \\ &\quad = \left(\frac{V_1 + V_2 + N_A + N_B}{2}\right)^2 \\ &\quad - \min_{r_A, r_B, \theta_A, \theta_B} \left[\left(\frac{V_2 - V_1}{2} - r_A \cos\theta_A - r_B \cos\theta_B\right)^2 \right. \\ &\qquad \left. +(-V_{12} - r_A \sin\theta_A - r_B \sin\theta_B)^2\right]. \end{aligned} \tag{56}$$

The second term on the right in (56) is the minimum squared distance between the points $((V_2 - V_1)/2, -V_{12})$ and $(r_A \cos\theta_A + r_B \cos\theta_B, \ r_A \sin\theta_A + r_B \sin\theta_B)$. If $((V_2 - V_1)/2, -V_{12})$ lies in the radius-$(N_A + N_B)/2$ circle that is centered at the origin, then the second term vanishes. Otherwise, a simple calculation gives this minimum distance. As a result we find that the maximum sum rate is,

$$R_{\max 12} = \max_{V_\alpha, V_\beta} S(\bar{\rho}_{AB}) - S(\hat{\rho}(0)) \tag{57}$$

$$= \begin{cases} g\left(V_1 + V_2 + N_A + N_B - \frac{1}{2}\right) - g\left(2|V|^{1/2} - \frac{1}{2}\right), \\ \qquad \text{for } N_A + N_B \geq ((V_1 - V_2)^2 + 4V_{12}^2)^{1/2} \\ g\left(2\left[[(V_1 + V_2 + N_A + N_B)/2]^2 - \left(\sqrt{[(V_1 - V_2)/2]^2 + V_{12}^2} - (N_A + N_B)/2\right)^2\right]^{1/2} - \frac{1}{2}\right) \\ \quad - g\left(2|V|^{1/2} - \frac{1}{2}\right), \\ \qquad \text{for } N_A + N_B < ((V_1 - V_2)^2 + 4V_{12}^2)^{1/2}. \end{cases} \tag{58}$$

We claim that the two-user capacity region for the HSH MAC with initial-state quadrature-component variance matrix $V$ and input constraints $N_A$ and $N_B$, is the region defined by the inequalities

$$R_1 \leq R_{\max 1}, \quad R_2 \leq R_{\max 2}, \quad \text{and} \quad R_{12} \leq R_{\max 12}. \tag{59}$$

To verify this claim, we will show that the corners of this region are achievable. The capacity region result then follows by time-sharing.

Let the point $((V_2 - V_1)/2, -V_{12})$ have coordinates $(r_V, \theta_V)$ and suppose that $N_B > N_A$. To show that the lower corner $(R_{\max 1}, R_{\max 12} - R_{\max 2})$ is achievable, we need to find points $(r_A, \theta_A)$ and $(r_B, \theta_B)$ that simultaneously minimize the distance between $(r_V, \theta_V)$ and $(r_A, \theta_A)$ and the distance between $(r_V, \theta_V)$ and $(r_A, \theta_A) + (r_B, \theta_B)$. Similarly, to show that the upper corner $(R_{\max 12} - R_{\max 1}, R_{\max 2})$ is achievable, we need to minimize the distance between $(r_V, \theta_V)$ and $(r_B, \theta_B)$ and the distance between $(r_V, \theta_V)$ and $(r_A, \theta_A) + (r_B, \theta_B)$. There are four cases to consider: see Fig. 3. For each case, we list the coordinates $(r_A, \theta_A)$ and $(r_B, \theta_B)$ corresponding to the capacity-achieving input distributions.

- Case I.
  - lower corner: $(r_A, \theta_A) = (r_V, \theta_V)$ and $(r_B, \theta_B) = (0, 0)$
  - upper corner: $(r_A, \theta_A) = (0, 0)$ and $(r_B, \theta_B) = (r_V, \theta_V)$
- Case II.
  - lower corner: $(r_A, \theta_A) = (N_A/2, \theta_V)$ and $(r_B, \theta_B) = (r_V - N_A/2, \theta_V)$
  - upper corner: $(r_A, \theta_A) = (0, 0)$ and $(r_B, \theta_B) = (r_V, \theta_V)$
- Case III.
  - lower corner: $(r_A, \theta_A) = (N_A/2, \theta_V)$ and $(r_B, \theta_B) = (r_V - N_A/2, \theta_V)$
  - upper corner: $(r_A, \theta_A) = (r_V - N_B/2, \theta_V)$ and $(r_B, \theta_B) = (N_B/2, \theta_V)$

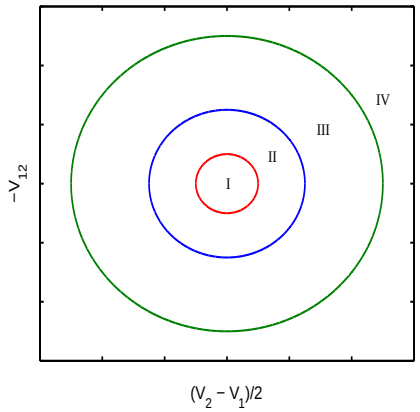


FIG. 3: (Color online) Regions used to complete the HSH MAC capacity-region proof. Case I: $r_V \leq N_A/2$. Case II: $N_A/2 < r_V \leq N_B/2$. Case III: $N_B/2 < r_V \leq (N_A + N_B)/2$. Case IV: $r_V > (N_A + N_B)/2$.

- Case IV.
  - lower corner: $(r_A, \theta_A) = (N_A/2, \theta_V)$ and $(r_B, \theta_B) = (N_B/2, \theta_V)$
  - upper corner: $(r_A, \theta_A) = (N_A/2, \theta_V)$ and $(r_B, \theta_B) = (N_B/2, \theta_V)$.

### B. Gaussian MAC Capacity

We now apply the capacity result derived in the previous section to the two-user optical MAC in Fig. 1. Alice and Bob encode their classical messages $\alpha$ and $\beta$ using input states of the form

$$\hat{\rho}_A(\alpha) = \hat{D}(\alpha)\hat{\rho}_A(0)\hat{D}^\dagger(\alpha) \tag{60}$$

$$\hat{\rho}_B(\beta) = \hat{D}(\beta)\hat{\rho}_B(0)\hat{D}^\dagger(\beta), \tag{61}$$

where $\hat{\rho}_A(0)$ and $\hat{\rho}_B(0)$ are zero-mean Gaussian states with quadrature-component covariance matrices $V_A$ and $V_B$, respectively. This is a modulation code for which the coherent-state encoding is the special case in which $\hat{\rho}_A(0)$

and $\hat{\rho}_B(0)$ are vacuum states. Charlie receives the output ensemble $\{p_A(\alpha)p_B(\beta),\ \mathcal{E}(\hat{\rho}_A(\alpha)\otimes\hat{\rho}_B(\beta))\}$, where the channel output $\mathcal{E}(\hat{\rho}_A(\alpha)\otimes\hat{\rho}_B(\beta))$ is the Gaussian state with mean $\sqrt{\eta}\,\alpha+\sqrt{1-\eta}\,\beta$ and covariance matrix $\eta V_A+(1-\eta)V_B$. The capacity of this Gaussian MAC, with input mean photon number constraints $\bar{n}_A$ and $\bar{n}_B$, is the HSH capacity region found in the previous section with

$$V = \eta V_A + (1-\eta)V_B, \tag{62}$$

$$N_A = \eta\big(\bar{n}_A - V_1^A - V_2^A + 1/2\big), \tag{63}$$

$$N_B = (1-\eta)\big(\bar{n}_B - V_1^B - V_2^B + 1/2\big). \tag{64}$$

For $\bar{n}_A$ and $\bar{n}_B$ sufficiently large, this capacity region is the set of rate pairs that satisfy

$$R_1 \leq g\big(\eta\bar{n}_A + (1-\eta)\left(V_1^B + V_2^B - 1/2\right)\big) - g\Big(2|V|^{1/2} - 1/2\Big), \tag{65a}$$

$$R_2 \leq g\big(\eta\left(V_1^A + V_2^A - 1/2\right) + (1-\eta)\bar{n}_B\big) - g\Big(2|V|^{1/2} - 1/2\Big), \tag{65b}$$

$$R_1 + R_2 \leq g(\eta\bar{n}_A + (1-\eta)\bar{n}_B) - g\Big(2|V|^{1/2} - 1/2\Big). \tag{65c}$$

When $V_A = V_B = I/4$, Alice's and Bob's initial states are vacuum states, hence they are employing coherent-state encoding and Eqs. (65) reduce to the coherent-state formulas in (11). As shown in Fig. 5, it is possible to find $V_A$ and $V_B$, for example,

$$V_A = V_B = \begin{pmatrix} 1/32 & 0 \\ 0 & 2 \end{pmatrix}, \tag{66}$$

when $\eta = 1/2$, $\bar{n}_A = 10$, and $\bar{n}_B = 8$, such that the Gaussian MAC capacity region is larger than the coherent-state MAC region. Numerical search over the space of possible covariance matrices is one way to further enlarge the capacity region beyond that achieved by this example. In the next section, we derive a result that implies the maximum individual rates achievable over the Gaussian MAC when Alice, say, is allowed to choose the optimal input covariance matrix $V_A$ corresponding to Bob's covariance matrix $V_B$. In Section V, we show that transmitting Gaussian states is asymptotically optimal in the limit of large $\bar{n}_A$ and $\bar{n}_B$.

## IV. ANISOTROPIC GAUSSIAN-NOISE CAPACITY

In this section, we generalize previous work [1, 2, 3, 4] on single-user lossy Bosonic channels with Gaussian excess noise to include anisotropic (colored) noise. In this section, the channel model we shall consider is the trace-preserving completely-positive (TPCP) map, $\mathcal{E}_\eta^{V_b}(\cdot)$, associated with the evolution from input mode $\hat{a}$ to output mode $\hat{c} = \sqrt{\eta}\,\hat{a} + \sqrt{1-\eta}\,\hat{b}$, when the noise mode, $\hat{b}$, is in a zero-mean Gaussian state, $\hat{\rho}_b$, with quadrature covariance matrix $V_b$. Let $\bar{n}_b$ denote the mean photon number of the Gaussian noise state $\hat{\rho}_b$.

In seeking the capacity of this channel, we shall *assume* that the conjecture about the minimum output entropy of the thermal-noise (isotropic-Gaussian noise) channel [4] is correct. This conjecture states that the minimum output entropy of the thermal-noise channel $\mathcal{E}(\cdot)$, which has $V_b = (2\bar{n}_T + 1)I/4$, where $I$ is the $2\times 2$ identity matrix, is given by

$$\min_{\hat{\rho}} S(\mathcal{E}(\hat{\rho})) = g((1-\eta)\bar{n}_T) \tag{67}$$

Presuming the correctness of this conjecture, we now have the following theorem.

**Theorem 1** *The classical capacity of the Gaussian-noise channel $\mathcal{E}_\eta^{V_b}$ is given by*

$$C = g(\eta\bar{n} + (1-\eta)\bar{n}_b) - g\left((1-\eta)\left(2|V_b|^{1/2} - 1/2\right)\right), \tag{68}$$

*for input mean photon numbers $\bar{n} \geq \bar{n}_{\rm thresh}$, where*

$$\bar{n}_{\rm thresh} = \frac{1}{\eta}\left((V_1' - V_2')^2 + 4V_{12}'^2\right)^{1/2} + V_1 + V_2 - \frac{1}{2}, \tag{69}$$

$$V' = \eta V + (1-\eta)V_b, \tag{70}$$

$$V = \frac{1}{4}\begin{pmatrix} |\mu+\nu|^2 & 2\,\mathrm{Im}(\mu\nu) \\ 2\,\mathrm{Im}(\mu\nu) & |\mu-\nu|^2 \end{pmatrix}, \tag{71}$$

*and the parameters $\mu$ and $\nu$ are chosen such that the squeeze operator $\hat{S}(z)$ whitens the Gaussian state $\hat{\rho}_b$.*

For sufficiently large input mean photon number $\bar{n}$, (68) gives the classical capacity of the single-user Gaussian-noise channel.

**Proof** We begin by establishing an upper bound on the capacity. By the HSW theorem,

$$C \leq \max_{\{p_j,\hat{\rho}_j\}} S\left(\sum_j p_j \mathcal{E}_\eta^{V_b}(\hat{\rho}_j)\right) - \min_{\{p_j,\hat{\rho}_j\}} \sum_j p_j S(\mathcal{E}_\eta^{V_b}(\hat{\rho}_j)) \tag{72}$$

$$\leq g(\eta\bar{n} + (1-\eta)\bar{n}_b) - \min_{\hat{\rho}_j} S(\mathcal{E}_\eta^{V_b}(\hat{\rho}_j)). \tag{73}$$

As sketched in Fig. 4, we can use the unitary squeeze operator $\hat{S}(z)$ to find a thermal-noise channel, with TPCP map $\mathcal{E}(\cdot)$, whose output minimum output entropy is equal to that of our anisotropic noise channel. [In essence, this is the quantum equivalent of the noise-whitening approach to communication through colored noise that is employed in classical communication theory.] The average noise-photon number, $\bar{n}_T$, of this equivalent channel is

$$\bar{n}_T = 2|V_b|^{1/2} - 1/2, \tag{74}$$

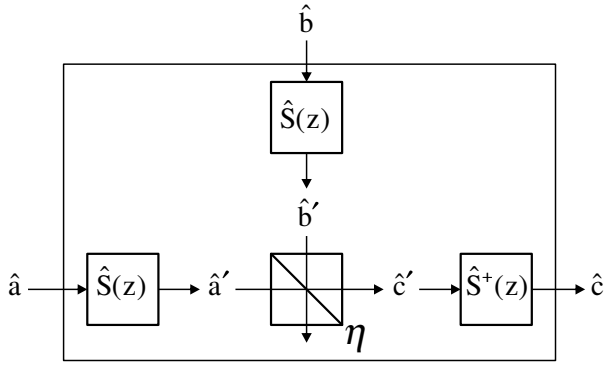


FIG. 4: Equivalent thermal-noise channel $\mathcal{E}_\eta^{\bar{n}_T}$ from $\hat{a}'$ to $\hat{c}'$. The input mode $\hat{a}'$ is in state $\hat{\rho}'$, and the noise operator $\hat{b}'$ is in a thermal state with mean photon number $\bar{n}_T = 2|V_b|^{1/2} - 1/2$. The original Gaussian-noise channel takes input $\hat{a}$ to output $\hat{c}$. For the squeeze operator $\hat{S}(z) \equiv \exp[(z^*\hat{a}^2 - z\hat{a}^{\dagger 2})/2]$, we use the parameterization $\mu = \cosh r$ and $\nu = e^{i\theta}\sinh r$, where $z = re^{i\theta}$. Squeezed vacuum states are defined as $|0;z\rangle \equiv \hat{S}(z)|0\rangle$.

which, when used in conjunction with (73) and our minimum output entropy conjecture, shows that the right-hand side of (68) is an upper bound on the channel capacity.

To show that the right-hand side of (68) is also a lower bound on the channel capacity when $\bar{n} \geq \bar{n}_{\rm thresh}$, we evaluate the information rate achieved by a single-use squeezed-state code. Let $\hat{\rho}_a^0 = |0;-z\rangle\langle 0;-z|$ be the zero-mean squeezed state whose quadrature-component covariance matrix is given by (71). Consider that random code in which we transmit the displaced squeezed states,

$$\hat{\rho}_a(\alpha) = \hat{D}(\alpha)\hat{\rho}_a^0\hat{D}^\dagger(\alpha), \tag{75}$$

that are selected with a zero-mean Gaussian probability density function whose quadrature-component covariance matrix is denoted $V_a$. Imposing the average photon number constraint, $\langle \hat{a}^\dagger\hat{a}\rangle \leq \bar{n}$, assuming that $\bar{n} \geq \bar{n}_{\rm thresh}$, and applying the HSH capacity result [11], we find that there is a squeezed-state code whose information rate equals the right-hand side of (36). This implies that

$$C \geq g(\eta\bar{n} + (1-\eta)\bar{n}_b) - g\left((1-\eta)\left(2|V_b|^{1/2} - 1/2\right)\right). \tag{76}$$

Equations (41) and (44) provide coincident upper and lower bounds on the capacity, when $\bar{n} \geq \bar{n}_{\rm thresh}$, hence the proof is complete.

There are two special cases of this theorem that are worth discussing. First, it is easy to see that when

$$V_b = \frac{2\bar{n}_b + 1}{4} I, \tag{77}$$

$\mathcal{E}_\eta^{V_b}$ reduces to the thermal-noise channel $\mathcal{E}$. Theorem 1 then predicts $\bar{n}_{\rm thresh} = 0$ and $C = g(\eta\bar{n} + (1-\eta)\bar{n}_T) - g((1-\eta)\bar{n}_T)$, in accord with the capacity conjecture for the thermal-noise channel [4]. A more interesting special case occurs when $\hat{\rho}_b = |0;z\rangle\langle 0;z|$ is a squeezed state, with $|\nu| > 0$, i.e., a pure-state anisotropic Gaussian noise. Here we find

$$V' = V = V_b = \frac{1}{4}\begin{pmatrix} |\mu-\nu|^2 & -2\,\mathrm{Im}(\mu\nu) \\ -2\,\mathrm{Im}(\mu\nu) & |\mu+\nu|^2 \end{pmatrix}, \tag{78}$$

which yields

$$C = g(\eta\bar{n} + (1-\eta)|\nu|^2), \tag{79}$$

for $\bar{n} \geq \bar{n}_{\rm thresh} = |\mu\nu|/\eta + |\nu|^2$. Note that this capacity is *higher* than that of the thermal-noise channel with the same $\bar{n}_b$ value. In other words, phase-sensitive, pure-state Gaussian noise enhances, rather than degrades channel capacity for $\bar{n} \geq \bar{n}_{\rm thresh}$.

## V. CAPACITY OUTER BOUND

Achieving the ultimate capacity region of the optical MAC may require the use of non-Gaussian states, so the capacity of the Gaussian MAC is still only an inner bound on this region. In this section, we develop an outer bound on the ultimate capacity region of the optical MAC. Let Alice and Bob use input states—averaged over their respective random-coding ensembles—$\bar{\rho}_A$ and $\bar{\rho}_B$ that are subject to the average photon number constraints $\bar{n}_A$ and $\bar{n}_B$. Because von Neumann entropy is invariant to mean fields, we know that the optimum $\bar{\rho}_A$ and $\bar{\rho}_B$ will be zero-mean-field states. This, in turn, implies that $\langle \hat{c}^\dagger\hat{c}\rangle = \eta\bar{n}_A + (1-\eta)\bar{n}_B$, from which it is easily shown that

$$R_1 + R_2 \leq S(\mathcal{E}(\bar{\rho}_A \otimes \bar{\rho}_B)) \leq g\left(\eta\bar{n}_A + (1-\eta)\bar{n}_B\right). \tag{80}$$

The sum-rate upper bound in (80) coincides with the coherent-state MAC result appearing in (11c). Hence, we have shown that the sum rate for the capacity region is achieved by coherent-state encoding in conjunction with optimum (joint-measurement) reception. More generally, the Gaussian-state encoding is a sum-rate-achieving code in the above-threshold regime, i.e., (65c) coincides with (80), whenever $\mathcal{E}(\rho_A(0) \otimes \rho_B(0))$ is pure. Moreover, from (6c) it can be shown that heterodyne reception is asymptotically optimum for the sum rate in the limit $\eta\bar{n}_A + (1-\eta)\bar{n}_B \to \infty$.

To upper bound the individual rates $R_1$ and $R_2$, consider a super receiver that has access to both output ports of the beam splitter representing the optical MAC. This super receiver can invert the unitary beam splitter transformation to undo the effects of the optical MAC. Thus, the individual rate upper bounds reduce to single-user Holevo informations, and we have the upper bounds $R_1 \leq g(\bar{n}_A)$ and $R_2 \leq g(\bar{n}_B)$. Our optical MAC results are illustrated in Fig. 5. Here we have plotted the sum rate for a two-user, single-mode, quantum optical MAC

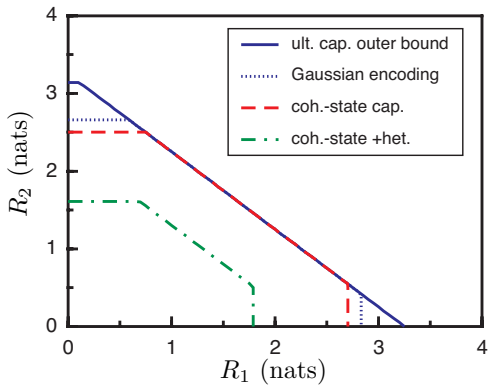


FIG. 5: (Color online) Ultimate capacity region of the two-user, single-mode optical MAC. Inner bounds from coherent-state and Gaussian-state encodings, and outer bounds given by $R_1 \leq g(\bar{n}_A)$, $R_2 \leq g(\bar{n}_B)$, and $R_1 + R_2 \leq g(\eta\bar{n}_A + (1-\eta)\bar{n}_B)$ are shown. The Gaussian-state capacity region is evaluated with input variance matrices $V_A$ and $V_B$ given by (66). This figure assumes $\eta = 1/2$, $\bar{n}_A = 10$, and $\bar{n}_B = 8$. Rates are measured in nats, i.e., logarithms are taken base $e$.

with $\eta = 1/2$, $\bar{n}_A = 10$, and $\bar{n}_B = 8$, along with the capacity region for heterodyne detection, the individual rate limits for coherent-state encoding, and the individual rate limits for the Gaussian-state encoding from Eq. (66).

We have presented codes which achieve the sum-rate upper bound, but it is unknown exactly how far we can reach into the corners of the outer bound region. One thing we can demonstrate is that the individual rate upper bounds are asymptotically achievable in the limit of large $\bar{n}_A$ and $\bar{n}_B$. Let Alice transmit real-valued classical messages $\alpha_1$ using squeezed states $|\alpha_1; z\rangle$ excited in the first quadrature with squeeze parameter $z > 0$. Let Bob transmit the zero-mean squeezed state $|0; Z\rangle$ with squeeze parameter $Z = \sinh^{-1}(\sqrt{\bar{n}_B})$, i.e., Bob squeezes as hard as possible, given his average photon number constraint. A rate of

$$R_1 = \frac{1}{2}\log\left(1 + \frac{4(\bar{n}_A - \sinh^2 z)}{e^{-2z} + (1-\eta)e^{-2Z}/\eta}\right) \tag{81}$$

is achieved if Charlie uses homodyne detection to decode Alice's message. After substituting in Alice's optimal value for her squeeze parameter, $z = \log(2\bar{n}_A + 1)/2$, and performing several applications of L'Hôpital's rule, we obtain the ratio

$$\begin{aligned}
&\lim_{\bar{n}_A\to\infty}\lim_{\bar{n}_B\to\infty}\frac{R_1}{g(\bar{n}_A)} \\
&\quad = \lim_{\bar{n}_A\to\infty}\frac{\frac{1}{2}\log\left(1 + 4e^{2z}(\bar{n}_A - \sinh^2 z)\right)}{g(\bar{n}_A)} &(82)\\
&\quad = \lim_{\bar{n}_A\to\infty}\frac{\log(1+2\bar{n}_A)}{g(\bar{n}_A)} &(83)\\
&\quad = 1. &(84)
\end{aligned}$$

Thus, this squeezed-state code with homodyne detection is asymptotically optimal for large input photon numbers $\bar{n}_A$ and $\bar{n}_B$. For the special case $\eta = 1$, Bob is irrelevant, and the above argument shows that the squeezed-state/homodyne code is asymptotically optimal for the single-user lossless Bosonic channel.

## VI. CONCLUSIONS

We have derived the capacity region of the Bosonic multiple-access channel that uses coherent-state encoding. Single-mode and wideband transmitters were considered, and in both cases optimum (joint measurements over entire codewords) reception was shown to outperform receivers that employed homodyne or heterodyne detection. Coherent-state encoding with optimum reception was shown to achieve the sum-rate bound on the ultimate capacity region of the optical MAC. In the limit of high average photon numbers, the ultimate single-user rates can be achieved with squeezed-state encoding and homodyne detection.

### Acknowledgments

This work was supported by the DoD Multidisciplinary University Research Initiative (MURI) program administered by the Army Research Office under Grant DAAD19–00-1–0177.

## APPENDIX

We apply the capacity theorem derived in [7] based on the following argument. Suppose that the transmitters used by Alice and Bob employ states containing no more than $K$ photons, where

$$K \gg \max\{1, \bar{n}_A + \bar{n}_B\}. \tag{A.1}$$

As their states may be indexed by complex-valued parameters $\alpha$ and $\beta$, over which we can do random coding, the result described by (1) specifies the achievable rate region within this restricted finite-dimensional state space. The right-hand sides of (1) — when maximized over product distributions that respect the $\bar{n}_A$ and $\bar{n}_B$ constraints — are monotonically expanding achievable rate regions with increasing $K$. Moreover, the achievable rate region for any $K$ is outer bounded by the results we derive in Section V assuming the full Hilbert space is employed. For fixed $\bar{n}_A$ and $\bar{n}_B$, the impact of the truncation to no more than $K$ photons will be negligible, under the condition (A.1), and will vanish as $K \to \infty$.

[1] V. Giovannetti, S. Guha, S. Lloyd, L. Maccone, J. H. Shapiro, and H. P. Yuen, Phys. Rev. Lett. **92**, 027902 (2004).

[2] V. Giovannetti, S. Guha, S. Lloyd, L. Maccone, J. H. Shapiro, B. J. Yen, and H. P. Yuen, Quantum Information and Computation **4**, 489 (2004).

[3] J. H. Shapiro, V. Giovannetti, S. Guha, S. Lloyd, L. Maccone, and B. J. Yen, in *Proceedings of the Seventh International Conference on Quantum Communication, Measurement and Computing*, edited by S. M. Barnett, E. Andersson, J. Jeffers, P. Öhberg, and O. Hirota (2004).

[4] V. Giovannetti, S. Guha, S. Lloyd, L. Maccone, and J. H. Shapiro, Phys. Rev. A **70**, 032315 (2004).

[5] B. J. Yen, *Multiple-user quantum optical communication* (2004), Research Laboratory of Electronics Technical Report 707, Massachusetts Institute of Technology.

[6] T. M. Cover and J. A. Thomas, *Elements of Information Theory* (John Wiley & Sons, New York, 1991).

[7] A. Winter, IEEE Trans. Inf. Theory **47**, 3059 (2001).

[8] A. S. Holevo, IEEE Trans. Inf. Theory **44**, 269 (1998).

[9] P. Hausladen, R. Jozsa, B. Schumacher, M. Westmoreland, and W. K. Wootters, Phys. Rev. A (1996).

[10] B. Schumacher and M. D. Westmoreland, Phys. Rev. A **56**, 131 (1997).

[11] A. S. Holevo, M. Sohma, and O. Hirota, Phys. Rev. A **59**, 1820 (1999).